

CORRECTION

Correction: Induction of nitric oxide synthase-2 proceeds with the concomitant downregulation of the endogenous caveolin levels (doi:10.1242/jcs.01002)

Inmaculada Navarro-Lérida, María Teresa Portolés, Alberto Álvarez Barrientos, Francisco Gavilanes, Lisardo Boscá and Ignacio Rodríguez-Crespo

This Correction updates and replaces the Expression of Concern (doi:10.1242/jcs.209981) relating to J. Cell Sci. (2004) 117, 1687-1697.

Journal of Cell Science was made aware of issues with this paper by a reader. Bands were duplicated in the caveolin-1 blot in Fig. 4A and NOS2 loading control blot in Fig. 6A. After discussion with the corresponding author, Ignacio Rodríguez-Crespo, we referred this matter to Universidad Complutense de Madrid (UCM). The UCM investigating committee reviewed replicate experiments to determine if they supported the scientific results and conclusions. They concluded that: "...despite the inadmissible manipulation in the production of the figures, the results and conclusions of the paper seem ultimately supported by the original experiments...".

The editorial policies of Journal of Cell Science state that: "Should an error appear in a published article that affects scientific meaning or author credibility but does not affect the overall results and conclusions of the paper, our policy is to publish a Correction..." and that a Retraction should be published when "...a published paper contain[s] one or more significant errors or inaccuracies that change the overall results and conclusions of the paper...". We follow the guidelines of the Committee on Publication Ethics (COPE), which state: "Retraction should usually be reserved for publications that are so seriously flawed (for whatever reason) that their findings or conclusions should not be relied upon". The standards of figure assembly and data presentation in this paper fall short of good scientific practice. However, given that the investigating committee at UCM decided that the conclusions of the paper were not affected by the errors, the appropriate course of action – according to COPE guidelines – is to publish a Correction, which the journal has made as detailed as possible.

Replicate data for the experiments shown in Fig. 4A and Fig. 6A were available and the correct figure panels are shown below. Note that results are presented in a different order in Fig. 4A compared with the original to avoid splicing of the blots.

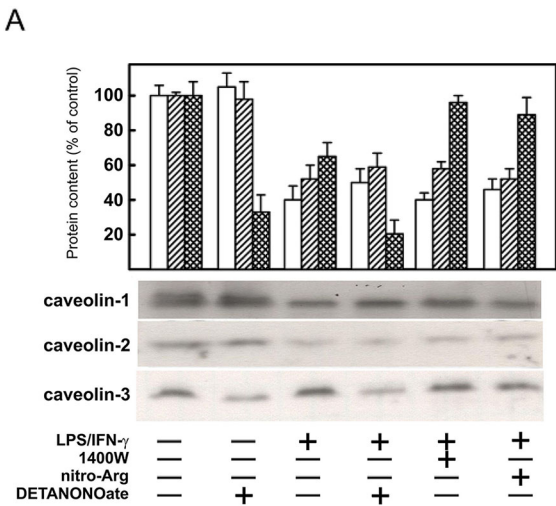


Fig. 4. Treatment of myotubes with ·NO donors induce changes in the levels of cav-3, but not of cav-1 or cav-2. C2C12 myoblasts were differentiated into myotubes and incubated with LPS (2 µg ml⁻¹) plus IFN-γ (100 U ml⁻¹), the ·NO donor DETA-NONOate (100 µM), the ·NO inhibitors 1400W (100 µM) and nitro-Arg (100 µM) for 36 h (cav-1 and cav-2) or 48 h (cav-3) in different combinations. The cells were scraped and the changes in cav-1 (white bars), cav-2 (single-slashed bars) and cav-3 (double-slashed bars) protein levels were determined by immunodetection (A).

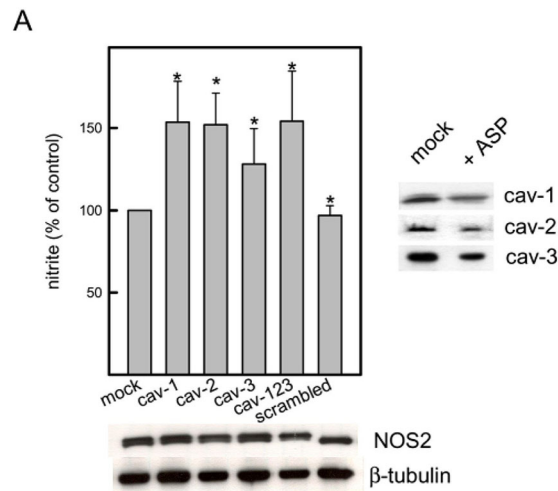


Fig. 6. Synthesis of \cdot NO in mouse C2C12 myotubes treated with LPS/IFN- γ when incubated with antisense phosphorothioates (ASP) of cav-1, cav-2 and cav-3 (A), and abrogation of caveolin-1 downregulation by protein kinase inhibitors (B). C2C12 myotubes were treated for 8 hours with antisense phosphorothioate oligonucleotides complementary to the first 21 bases of the mRNA encoding cav-1, cav-2 and cav-3. After the treatment, the muscle cells were challenged with LPS/IFN- γ for 36 hours and the amount of \cdot NO that accumulates was determined with the Griess assay. The antisense oligonucleotides (ASP) were added individually (cav-1, cav-2 and cav-3) or in combination (cav-123). A scrambled oligo corresponding to the cav-1 base sequence was also used as a control. The absence of changes in NOS2 and β -tubulin in each case is confirmed by immunodetection (A, bottom). The results shown are representative of ten individual experiments.

The authors apologise to the journal and readers for these errors.

Journal of Cell Science refers readers to other Corrections related to the UCM investigation:

doi:10.1242/jcs.219634

doi:10.1242/jcs.219675

doi:10.1242/jcs.219683

Induction of nitric oxide synthase-2 proceeds with the concomitant downregulation of the endogenous caveolin levels

Inmaculada Navarro-Lérda¹, María Teresa Portolés¹, Alberto Álvarez Barrientos², Francisco Gavilanes¹, Lisardo Boscá^{2,3} and Ignacio Rodríguez-Crespo^{1,*}

¹Departamento de Bioquímica y Biología Molecular, Facultad de Ciencias Químicas, Universidad Complutense, 28040 Madrid, Spain

²Fundación Centro Nacional de Investigaciones Cardiovasculares, Madrid, Spain

³Instituto de Bioquímica (Centro Mixto Consejo Superior de Investigaciones Científicas-UCM), Facultad de Farmacia, Universidad Complutense, 28040 Madrid, Spain

*Author for correspondence (e-mail: nacho@bbm1.ucm.es)

Accepted 20 November 2003

Journal of Cell Science 117, 1687–1697 Published by The Company of Biologists 2004
doi:10.1242/jcs.01002

Summary

Several cell types express inducible nitric oxide synthase (NOS2) in response to exogenous insults such as bacterial lipopolysaccharide (LPS) or proinflammatory cytokines. For instance, muscular cells treated with LPS and interferon γ (IFN- γ) respond by increasing the mRNA and protein levels of NOS2, and synthesize large amounts of nitric oxide. We show here that transcriptional induction of NOS2 in muscular cells proceeds with a concomitant decrease in the levels of caveolin-1, -2 and -3. Addition of \cdot NO-releasing compounds to C2C12 muscle cells reveals that this downregulation of the caveolin (cav) levels is due to the presence of \cdot NO itself in the case of caveolin-3 and to the action of the LPS/IFN- γ in the case of cav-1 and cav-2. Likewise, muscle cells obtained from NOS2^{-/-} knockout mice challenged with LPS/IFN- γ could downregulate their levels of cav-1 but not of cav-3, unlike wild-type animals, in

which both cav-1 and cav-3 levels diminished in the presence of the proinflammatory insult. Laser confocal immunofluorescence analysis proves that \cdot NO exerts autocrine and paracrine actions, hence diminishing the cav-3 levels. When the induced NOS2 was purified using an affinity resin or immunoprecipitated from muscular tissues, it appears strongly bound not only to calmodulin but also to cav-1, and marginally to cav-2 and cav-3. When the cav levels were reduced using antisense oligonucleotides, an increase in the NOS2-derived \cdot NO levels could be measured, demonstrating the inhibitory role of the three cav isoforms. Our results show that cells expressing NOS2 diminish their cav levels when the synthesis of \cdot NO is required.

Key words: Nitric oxide, Caveolin, Muscle, Inflammation

Introduction

The gaseous radical nitric oxide (\cdot NO) modulates biological function in a wide range of tissue types, acting either as a signalling molecule or as a toxin. Cellular \cdot NO production is mediated by the nitric oxide synthases (NOSs), enzymes that use O₂ and NADPH as substrates to convert the amino acid L-arginine into L-citrulline, and release NADP⁺ and \cdot NO. Three human NOS isoforms have been cloned and characterized. NOS2 (sometimes referred to as inducible NOS or iNOS) is mostly involved in the synthesis of the large amounts of \cdot NO that appear in inflammatory and immunological processes (MacMicking et al., 1997). Binding of calmodulin (CaM) to the interdomain hinge of all NOS isoforms activates the electron transfer from the flavins to the heme required for \cdot NO production. Unlike NOS1 and NOS3, the irreversible binding of CaM to NOS2 is essentially independent of the intracellular Ca²⁺ concentrations, and it is generally assumed that CaM binds to NOS2 co-translationally and in a 1:1 molar ratio (MacMicking et al., 1997; Cho et al., 1992).

NOS2 was initially described in activated macrophages as an enzyme involved in mechanisms of cytotoxicity (Hibbs et al., 1988). This isoform is not usually expressed in healthy

quiescent cells but it is rapidly transcriptionally induced in response to stimulation with bacterial endotoxins [lipopolysaccharide (LPS)] or proinflammatory cytokines in multiple cellular types. The NOS2-derived \cdot NO is important for killing and host defense against certain protozoa, bacteria, fungi and viruses (Bogdan, 2001). Although the generation of \cdot NO is a feature of genuine immune-system cells (natural killer cells, mast cells, dendritic cells, microglia, Kupffer cells, neutrophils and eosinophils), expression of NOS2 is equally observed in other cell types, such as epithelial cells, fibroblasts, hepatocytes and keratinocytes, in response to various proinflammatory stresses (Bogdan, 2001). Interestingly, although NOS2 is usually considered in terms of physiopathological processes, studies with NOS2 knockout mice have indicated several physiological roles for the NOS2-generated \cdot NO, for example in osteoclastic bone resorption (van't Hof et al., 2000).

Within cells, it is not only CaM that interacts with NOS2. Using the yeast two-hybrid approach, three more cellular proteins that bind to NOS2 have been identified: kalirin, NAP110 (both binding to the first 70 amino acids of NOS2) and Rac (binding to the oxygenase domain) (Ratovitski et al., 1999a; Ratovitski et al., 1999b; Kuncewicz et al., 2001).

Kalirin is a cytosolic protein with nine spectrin-like repeats that inhibits NOS2 by preventing the formation of the active homodimers (Ratovitski et al., 1999a). NAP110 is a membrane-bound macrophage protein that also promotes the dimer-to-monomer conversion of NOS2, resulting in the loss of enzymatic activity (Ratovitski et al., 1999b). Finally, Rac, a member of the Rho GTPase family, binds to NOS2 and, upon overexpression, slightly increases the enzymatic synthesis of \cdot NO (Kuncewicz et al., 2001).

Interaction of NOS1, NOS2 and NOS3 with some of the three caveolin (cav) isoforms has also been reported. In this context, the process involving the interaction of cav-1 with NOS3 (eNOS) is undoubtedly the best characterized. Reports from the laboratories of Michel and Sessa have established a model in which, in endothelial cells, myristoylated and doubly palmitoylated NOS3 translocates from the cytosol towards low-fluidity subdomains enriched in cav-1. As a consequence of this new localization, a direct inhibitory interaction between NOS3 and cav-1 residues 82-101 occurs that ultimately discontinues the \cdot NO synthesis. Because this process takes place when the intracellular calcium concentration is low, CaM is released from the hinge region that connects both domains of NOS3. This model also envisages a self-excluding regulatory cycle between cav-1 and CaM when binding to NOS3. When the intracellular calcium concentration increases, NOS3 becomes de-palmitoylated, cav-1 is released and CaM binds again (Gratton et al., 2000; Feron et al., 1998).

However, less is known about the interaction of NOS2 with caveolin isoforms, despite the fact that they are abundantly expressed in cell types in which NOS2 is expressed in response to inflammatory stimuli. Additionally, it is not clear whether certain post-translational modifications occur on NOS2 that favor its redistribution to membranous subdomains, where the interaction with caveolin might take place. For instance, in Raw 264.7 macrophages, antibodies raised against the first 17 amino acids of NOS2 were able to react with a cytosolic but not with a membrane-bound form of NOS2, whereas antibodies that recognize the C-terminus of NOS2 recognized both the soluble and membrane-associated NOS2 (Ringheim and Pan, 1995). Significantly, primary cultures of activated mouse macrophages also displayed a subpopulation of NOS2 that remained membrane-bound (Vodovotz et al., 1995) and in slow-twitch fibers of guinea-pig skeletal muscle NOS2 immunoreactivity was found almost exclusively in the particulate fraction (Gath et al., 1996). However, it remains to be established whether the membrane-bound subpopulation of NOS2 associates with caveolin and whether this interaction leads to its enzymatic inhibition. In this regard, a recent report has described that the ectopic expression of cav-1 in carcinoma cell lines results in the translocation of NOS2 to Triton-X-100-insoluble subdomains termed caveolae, where it becomes degraded via the proteasome pathway (Folley-Bosco et al., 2000). The possibility therefore exists that cav-1 interacts with NOS2 and regulates its activity. In agreement with this observation, incubation of purified NOS2 with the 'scaffolding domain' peptide of both cav-1 (residues 82-101) and cav-3 (residues 55-74) completely abrogated \cdot NO synthesis by NOS2 (García-Cardena et al., 1997). Hence, the intriguing possibility of CaM-bound NOS2 physiologically interacting with and being regulated by cav-1 in a ternary complex remains unexplored.

In this work, we have primarily focused on skeletal muscle

cells, because they represent a well-established model of NOS2 induction in response to proinflammatory stimuli. Although NOS2 is expressed at low levels in normal human skeletal muscle (Park et al., 1996; Tews et al., 1998), its gene expression is significantly increased in patients with severe or chronic heart failure (Riede et al., 1998). Although both immunohistochemistry (Gath et al., 1999) and immunogold labeling (Adams et al., 1999) localized NOS2 predominantly over the myofibrils of skeletal muscle, other reports unambiguously localize NOS2 only at the sarcolemma (the plasma membrane of the muscle cell) (Tews et al., 1998). Additionally, in C2C12 skeletal muscle cells, NOS2 immunoprecipitates with the sarcolemmal membrane protein cav-3 (Gath et al., 1999), probably providing a molecular basis for the localization of NOS2 to the sarcolemma of muscle cells observed in certain studies. Here, we report that proinflammatory stimuli induce the appearance of NOS2 in muscle cells with a concomitant decrease in the caveolin levels, probably allowing the enzyme to reach full activity. Furthermore, the released \cdot NO acts in an autocrine and paracrine fashion, and diminishes the amount of the cav-3 that is present in neighboring cells.

Materials and Methods

Cell culture and materials

Glutamine, antibiotics, cell culture media [Dulbecco's modified Eagle medium (DMEM)], sulfanilic acid (4-amino-benzenesulfonic acid), NEDA [*N*-(1-naphthyl) ethylenediamine dihydrochloride], nitro-arginine, LPS (from *Salmonella enteritidis*), transfection reagents Escort-III and Escort-IV, 2',5'-ADP (adenylic acid) and Hoechst 3342 were purchased from Sigma. Trypsin-EDTA and fetal bovine serum (FBS) were from Bio Whittaker Europe. The sources of the various antibodies used in this work are: anti-NOS2 polyclonal serum (N32030), anti-cav-1 polyclonal serum (C13630), anti-cav-1 monoclonals (clone 2234 and 060), anti-cav-2 monoclonal (clone 65) and anti-cav-3 monoclonal (clone 26) were from Transduction Laboratories; anti- β -tubulin-I (T7816) monoclonal antibody, anti-CaM monoclonal antibody (clone 6D4) and anti-NOS2 monoclonal antibody (N9657) were purchased from Sigma. Recombinant human interferon γ (IFN- γ) was from PeproTech. DETA NONOate {[Z]-1-[*N*-(2-aminoethyl)-*N*-(2-ammonioethyl)amino] diazen-1-ium-1,2-diolate} and 1400W dihydrochloride {[*N*-(3-(aminomethyl)benzyl]acetamidine)} were from Cayman Chemicals. Protein-A/Sepharose, 2',5'-ADP/Sepharose, ECL reagents, Cy2- and Cy3-labelled secondary antibodies were from Amersham Biosciences. Antisense phosphorothioates were from Sigma-Genosys. NOS2 knockout mice (B6.129P2 and C57BL/6J000664 control strain) were obtained from Jackson Laboratories (Bar Harbor, ME). The protein kinase inhibitors were obtained from Calbiochem. BODIPY Texas Red ceramide was from Molecular Probes.

C2C12 mouse myoblasts were kindly provided by M. Lorenzo (Universidad Complutense de Madrid). The myoblasts were grown in DMEM supplemented with 10% FBS, 100 U ml⁻¹ penicillin, 100 μ g ml⁻¹ streptomycin and 2 mM L-glutamine in a 5% CO₂ atmosphere at 37°C. Differentiation of ~70% confluent myoblasts into myotubes was performed in DMEM supplemented with antibiotics and glutamine plus 50 nM insulin in the absence of serum for 3 days (Conejo et al., 2001). Myotubes (muscular cells) are characterized by the formation of elongated, multinucleated tubules that express cav-3. After the formation of the myotubes, the cells were incubated overnight with DMEM in the presence of 10% serum before adding the LPS/IFN- γ . To induce NOS2 expression in C2C12 myotubes, LPS (2 μ g ml⁻¹) plus IFN- γ (100 U ml⁻¹) was added in the presence of

DMEM and 10% FBS. The supernatant and the cells were collected at different times and analysed.

Determination of the \cdot NO release

Because nitric oxide decomposes to nitrites and nitrates, we determined the concentration of nitrites in the samples using the Griess assay. A 0.5 ml sample was incubated with 50 μ l of a 100 mM sulfanilic acid solution and 50 μ l of a 10 mM NEDA solution. The mixture was allowed to react for 15 minutes and then the absorbance value at 540 nm was determined. Every sample was analyzed in triplicate. Fresh solutions of sodium nitrite were regularly prepared as standards.

Depletion of endogenous cav-1, cav-2 and cav-3 using antisense phosphorothioates

We designed three 21-bp antisense phosphorothioates that annealed starting at the first ATG codon (initiation Met) of the *cav-1*, *cav-2* and *cav-3* mRNAs. Antisense phosphorothioate oligonucleotides (7.5 μ M) were transfected into C2C12 myotubes using Escort transfection reagent (Sigma) for 8 hours in DMEM in the absence of serum. Afterwards, the transfection mixture was removed, the cells were washed with DMEM with 10% FBS and the myotubes were challenged with LPS/IFN- γ for 36 hours. After this, the medium was collected and the \cdot NO synthesis was determined using the Griess assay. Likewise, the cells were scraped and harvested in order to immunodetect caveolin levels within them. Because the oligonucleotides tended to precipitate during the transfection process, resulting in variable transfection efficiencies, ten independent experiments of endogenous caveolin depletion were performed.

Construction of the NOS2-GFP plasmid

We PCR amplified the NOS2 cDNA (original clone from C. Nathan, Weill Medical College of Cornell University, New York) introducing a novel *NcoI* site at the 5' end and a novel *BssHII* site at the 3' end. The general design of the mutant consisted of NOS2 cDNA fused to the enhanced green fluorescent protein (GFP) using a *BssHII* site in the pCDNA3 plasmid (Invitrogen) under the control of the cytomegalovirus promoter, as previously described (Navarro-Lérida et al., 2002). The PCR-amplified band was then ligated into the pGEM-T vector (Invitrogen) and subsequently sequenced. We then double digested the NOS2 in pGEM-T with *NcoI* plus *BssHII* and ligated this band into the corresponding sites of a pUC-linker-GFP construct that we had previously obtained (Navarro-Lérida et al., 2002). In this construct, we had a *BssHII* at the 5' end of the GFP coding region, as well as a *XhoI* at the 3' end followed by a hexa-His ending with a *XbaI* site. This NOS2-GFP pUC construct was digested with *XbaI* for 2 hours and *EcoRI* was then added for 5 minutes in order to induce a partial digestion (there are internal *EcoRI* sites within the NOS2 cDNA). Finally, the larger band obtained from this partial digestion (~4.2 kb) was ligated into pCDNA3 that had been previously digested with *EcoRI* plus *XbaI*. This NOS2-GFP pCDNA3 plasmid was used to transfect myoblasts and myocytes in culture using Escort-III and Escort-IV (Sigma) following the manufacturer's instructions.

Induction of NOS2 expression in wild-type and knockout mice

Mice were injected intraperitoneally with LPS (1.5 μ g LPS g⁻¹) and IFN- γ (8 U g⁻¹). PBS was injected into control animals in every experiment. After 16 hours, the animals were sedated, sacrificed and an extract of muscle (quadriceps) and liver obtained. A minimum of four mice were used in every condition.

Inhibition of cellular protein kinases

C2C12 myotubes were incubated with LPS/IFN- γ in the presence of

various protein kinase inhibitors. We tested wortmannin (200 nM), LY 294002 (20 μ M), SB 203580 (5 μ M), PD 98059 (10 μ M) and genistein (10 μ M). 36 hours after the activation, both the supernatant and the cells were harvested and the levels of cav-1 and cav-2 determined by immunoblotting. The concentration of nitrites in the supernatant was determined using the Griess assay as previously described.

Immunoblot analysis and cellular fractionation

Cellular proteins were resolved by either 7% or 15% acrylamide sodium-dodecyl-sulfate polyacrylamide-gel electrophoresis (SDS-PAGE) and transferred to nitrocellulose membranes. Western blots were incubated for 2 hours in PBS containing 2% powdered skim milk. Subsequently, the nitrocellulose membranes were incubated overnight with the primary antibodies (typically 1:1000 in PBS), washed and finally incubated for 2 hours with a horseradish-peroxidase-conjugated goat anti-rabbit antibody (Pierce).

Detection was performed using an ECL detection kit (Amersham Biosciences). Quantification of the intensity of the bands was performed using the UViband V97 software (UVItec St John's Innovation Centre, Cambridge, UK).

Fractionation was performed by harvesting the C2C12 myotubes treated with LPS/IFN- γ for 36 hours and resuspending them in 0.4 ml PBS supplemented with 1 mM EDTA, 10 μ g ml⁻¹ aprotinin, 10 μ g ml⁻¹ leupeptin, 2 μ M phenylmethylsulfonyl fluoride (Sigma) as protease inhibitors. The cellular suspensions were then passed several times through a syringe (0.5 \times 16 mm) on ice. Unbroken cells and cellular debris were eliminated by a 10-minute centrifugation at 5000 rpm in a tabletop microcentrifuge. The samples were then centrifuged for 1 hour at 200,000 g in an SW65 rotor (Beckman) at 4°C as previously described (Navarro-Lérida et al., 2002). The cellular pellets (particulate fraction) and the supernatants (soluble fraction) were brought to equal volumes and subsequently analysed by SDS-PAGE followed by immunodetection with the indicated antibodies.

Immunoprecipitation and purification of NOS2 from muscle

C2C12 myotubes treated for 36 hours with LPS/IFN- γ were washed with PBS, scrapped and lysed in Ripa buffer (10 mM Tris, 150 mM NaCl, 1% Triton X-100, 0.1% SDS, 0.1% deoxycholate, pH 7.35) in the presence of protease inhibitors. After centrifugation of the cell lysate at 6000 g for 10 minutes at 4°C, the supernatant was precleared with 20 μ l of Sepharose:Protein-A/Sepharose beads (Amersham Biosciences) in the absence of any added antibody for 1 hour at 4°C. The sample was spun and the beads removed. Afterwards, 5 μ l of the rabbit anti-NOS2 antibody were added to the sample and the mixture was incubated overnight at 4°C. Then, 25 μ l of a 1:1 Sepharose:Protein-A/Sepharose suspension were added to each sample and the incubation was maintained for 5 hours at 4°C. Immunoprecipitates were centrifuged at 15,000 rpm in a tabletop microcentrifuge for 10 minutes and the supernatant was removed. Samples were washed once with PBS to remove non-specific interactions, spun again and separated by SDS-PAGE, transferred to a membrane and immunodetected with the desired antibody.

NOS2 was purified using 40 plates of confluent C2C12 myotubes treated with LPS/IFN- γ for 36 hours as the starting material by means of a 2',5'-ADP/Sepharose affinity chromatography. The purification steps are similar to those previously reported (Rodríguez-Crespo et al., 1999) with the sole exception that the elution from the affinity column was performed with 25 mM 2',5'-ADP. The purified NOS2 was extensively dialysed against 100 mM (NH₄)HCO₃, pH 8.5, and then lyophilized.

Confocal fluorescence microscopy

Cells grown on 0.2% gelatin-coated glass coverslips were washed two

times with PBS and fixed for 15 minutes at room temperature with freshly prepared 2% paraformaldehyde in PBS. The stock paraformaldehyde solution was prepared at 4% in PBS and was centrifuged at 15,000 rpm for 5 minutes at room temperature in a table-top microcentrifuge in order to remove insoluble material before dilution. After removal of the 2% paraformaldehyde solution, the cells were washed with PBS and incubated with cold methanol at -20°C for 10 additional minutes. The methanol was removed and the coverslips were allowed to dry for 5 minutes. Then, the cells were washed with PBS and incubated with the desired primary antibodies at 37°C . In general, an overnight incubation was performed with the primary antibodies at a 1:200 dilution in a wet chamber followed by a 2 hour incubation with the secondary antibody. Finally, the slides were mounted using Fluoroguard anti-fade reagent (BioRad). The subcellular localization was observed under a BioRad Radiance 2100 confocal microscope, using the excitation wavelength of 405 nm for the Hoechst fluorescence (nuclear staining), 488 nm for the Cy2 fluorescence and 543 nm for the Cy3 fluorophore. A 60 \times oil-immersion objective was used. Analysis of the pictures was performed with the Confocal Assistant software (free software by T. Clark, version 4.02, <http://www.cyto.purdue.edu>) as well as with Laserpixmap and Lasersnap software from BioRad. Treatment of live cells with the Golgi marker BODIPY-Texas Red ceramide was performed as previously described (Navarro-Lérida et al., 2002).

Results

Proinflammatory stimuli upregulate NOS2 and downregulate caveolin levels in muscle cells

Mouse C2C12 myotubes are known to induce NOS2 transcriptionally in response to bacterial LPS and IFN- γ , so we first determined whether these stimuli could also affect the caveolin levels (Fig. 1). A low level of NOS2 can be observed in myotubes under basal conditions. As expected, addition of $2\text{ }\mu\text{g ml}^{-1}$ LPS plus 100 U ml^{-1} IFN- γ to mouse C2C12 myotubes results in the transcriptional induction of NOS2 with the consequent synthesis of large amounts of $\cdot\text{NO}$ that accumulate in the culture medium. The amount of NOS2 that can be immunodetected in C2C12 myotubes steadily increases up to 30 hours of treatment, and the released $\cdot\text{NO}$ (measured as accumulated nitrites) follows a similar pattern (Fig. 1A). However, when we determined the levels of cav-1, cav-2 and cav-3 that were present in myotubes under these circumstances, we observed a progressive diminution of the protein levels of all of them (Fig. 1B). The cav-1 protein (continuous line in Fig. 1B) becomes downregulated promptly, reaching about 55% of the initial levels after 24 hours of treatment with the cytokines, and about 28% of the initial levels after 48 hours of treatment. The cav-2 protein levels diminish as well (dotted line), with half of the total cellular protein levels being lost after 48 hours of treatment. Reduction in cav-3, the muscle-specific isoform, is equally observed (dashed line), although somehow more retarded with time. After 48 hours of incubation with LPS/IFN- γ , 65% of the initial protein content of cav-3 is still present, falling down to 37% after 56 hours of treatment. Hence, when the C2C12 myotubes transcriptionally increase their NOS2 levels, a concomitant decrease in the caveolin levels are observed.

Subcellular localization of NOS2 and cav-1, cav-2 and cav-3 in C2C12 myotubes

Next, we decided to investigate the intracellular distribution of

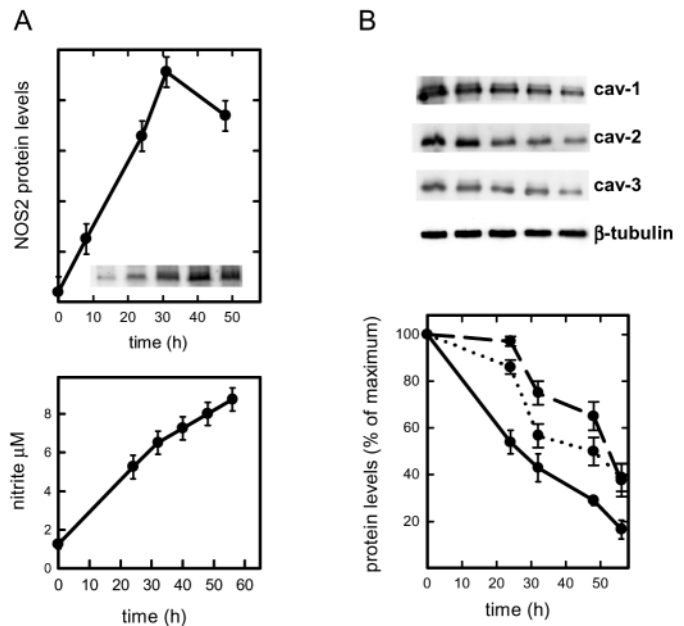


Fig. 1. Induction of NOS2 proceeds with the concomitant downregulation of the cav-1, cav-2 and cav-3 levels in mouse C2C12 myotubes treated with LPS/IFN- γ . Myotubes were treated with LPS/IFN- γ and the changes in NOS2, cav-1, cav-2 and cav-3 were analysed by immunoblot and quantified using the UVI-band software. Induction of NOS2 together with the accumulation of nitrites is depicted in (A). The intensity of the NOS2 bands at five different times as integrated using the UVI-band software is shown at the top. Accumulated nitrites in a 54 hour period is shown at the bottom. The disappearance of cav-1 (continuous line), cav-2 (dotted line) and cav-3 (dashed line) in myotubes is represented in (B), both as the immunodetected bands (top) and as a plot (bottom). Protein levels are expressed as percentage of the maximum; the initial amount of caveolin is therefore 100%. β -Tubulin is also shown as a control of total protein in each sample. The results shown are representative of four experiments (means \pm s.d.).

NOS2 and its putative overlap with the caveolin isoforms (Fig. 2). In untreated myotubes, cav-1, cav-2 and cav-3 strongly label the sarcolemma (plasma membrane), although, in agreement with previous observations (Luetterforst et al., 1999), it also localizes to intracellular membranes, most likely the Golgi apparatus (Fig. 2A, left). No nuclear distribution of caveolin was observed in any case. In the absence of proinflammatory stimuli, the amount of NOS2 immunodetected in C2C12 myotubes is very low, almost non-existent (Fig. 2A, middle). Upon treatment of these cells with LPS/IFN- γ for 36 hours, a clear cytosolic NOS2 staining could be observed (Fig. 2B). The caveolin staining becomes not only reduced but also non-uniform along any microscope field, and the overlap between NOS2 and caveolin-1 is found mostly in intracellular membranes within the sarcoplasm (yellow staining). The intracellular localization of NOS2 extends throughout the cytoplasm and becomes extinguished in the proximity of the sarcolemma. Overlap of cav-2 and NOS2 is less obvious than in the case of cav-1, whereas no overlap between cav-3 and NOS2 could be observed in stimulated cells (Fig. 2B). Detailed observation of the NOS2 distribution with a higher magnification reveals that, in certain subcellular

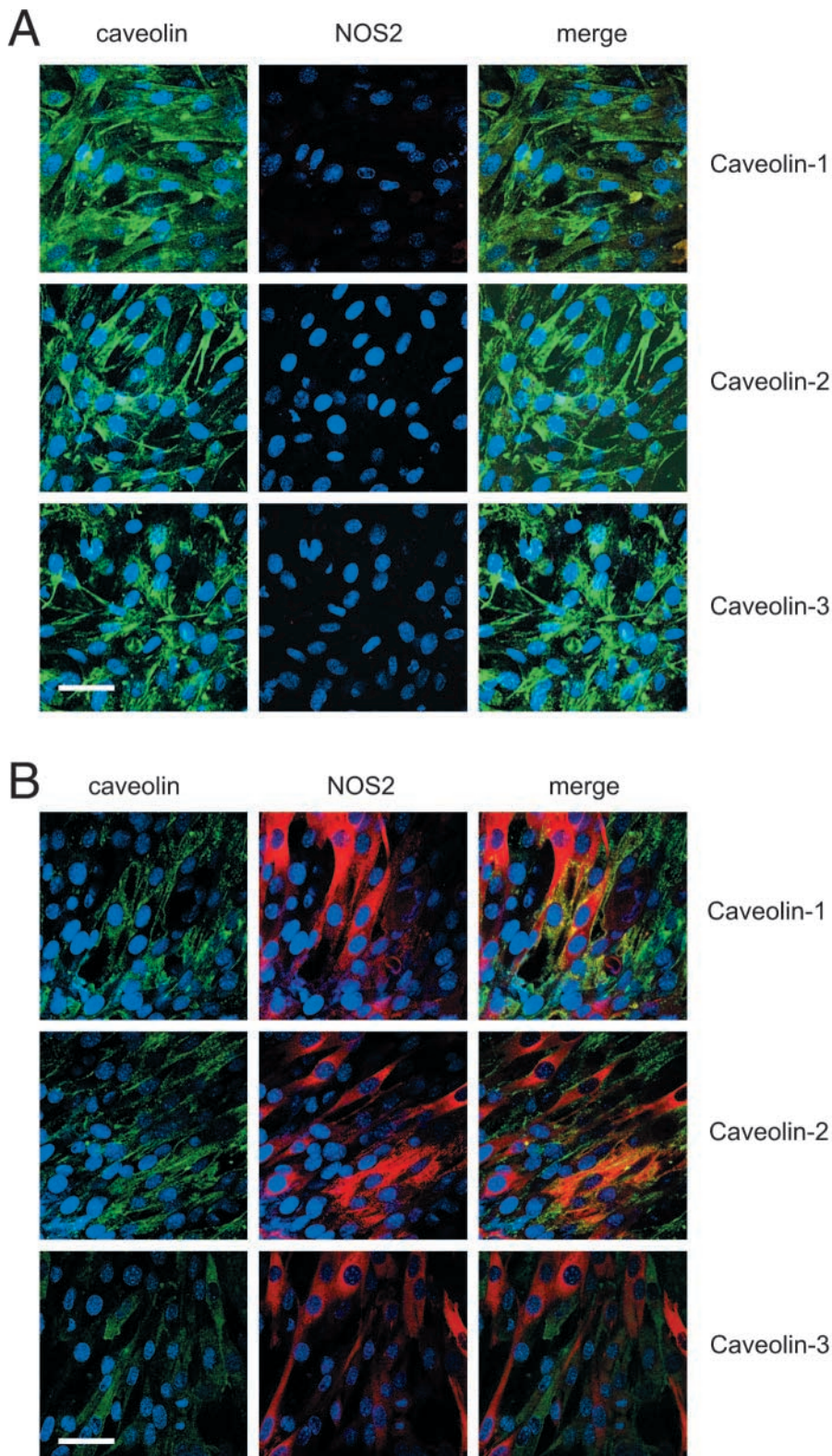


Fig. 2. Subcellular localization of NOS2 and the various caveolin isoforms in mouse C2C12 myotubes in control experiments (A) and in cells treated with the proinflammatory mixture of LPS/IFN- β (B). (Left) Myotubes were fixed with paraformaldehyde and methanol, and incubated with antibodies against cav-1, cav-2, cav-3 or NOS2 and either left untreated (A) or treated with LPS/IFN- γ for 36 hours (B). (Middle) Subcellular distribution of NOS2 in myotubes untreated (A) or treated with LPS/IFN- γ for 36 hours (B). The merge signal is depicted on the right. The caveolin fluorescence was visualized by confocal microscopy at an excitation wavelength of 488 nm and is shown in green, whereas the NOS2 was obtained after excitation at 543 nm and is shown in red. Overlap of green and red labeling is depicted in yellow; overlap of green and blue labeling is depicted in light blue; overlap of red and blue is depicted in violet. Scale bar, 50 μ M. In all cases, the position of the cell nuclei (blue) was obtained after staining with Hoechst and excitation at 405 nm.

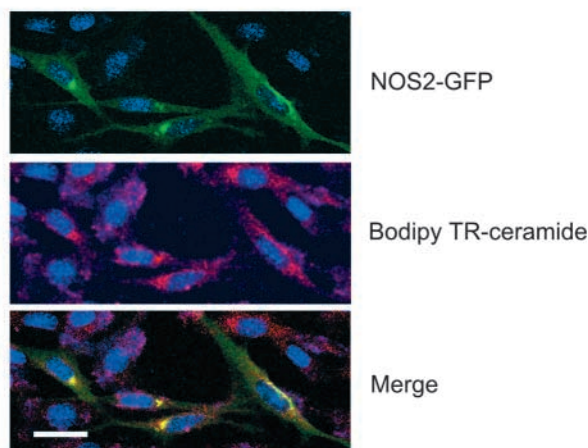
It is likewise remarkable that any myotube that rapidly responds to the proinflammatory cytokines and induces NOS2 expression eventually downregulates the levels of caveolin, specifically suggesting that NOS2 and caveolin expression are mutually exclusive at long times. This seems to be a common phenomenon for all cav-1, cav-2 and cav-3. Still, certain individual cells seem not to respond to the LPS/IFN- γ stimulus. Hence, even after 48 hours of treatment, certain cells in the culture (approximately 15% of the total) seem not to respond to the stimuli.

Because the amount of cav-1, cav-2 and cav-3 decrease in C2C12 myotubes after treatment with the mixture of LPS and IFN- γ , we investigated the distribution of NOS2 under situations of abundant caveolin presence (Fig. 3). Myoblasts were stained with the Golgi marker BODIPY Texas red ceramide *in vivo*, as previously reported (Navarro-Lérida et al., 2002). A very significant co-localization of NOS2 and BODIPY Texas red ceramide was apparent in perinuclear Golgi regions of the cell (Fig. 3A), which are probably enriched in caveolin (Luetterforst et al., 1999; Navarro-Lérida et al., 2002).

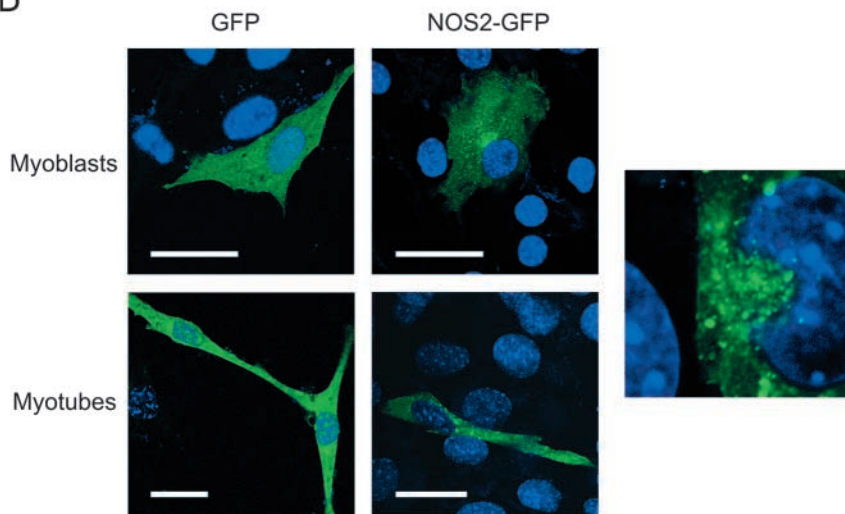
Transfection of myoblasts and myotubes with the reporter GFP plasmid resulted in the distribution of the fluorescence in the cytosol and the cell nucleus (Fig. 3B, left). However, the distribution of a NOS2-GFP construct in both myoblasts and unactivated myotubes is punctate in perinuclear areas and in the sarcolemma, clearly indicating that, when caveolin is

structures, it is not evenly distributed but instead repeatedly constitutes aggregated structures (see below). In the cells that simultaneously express NOS2 and caveolin, colocalization can be observed in certain membranous structures of the cytosol. Other activated cells limit their caveolin staining to the sarcolemma, with NOS2 being found all over the sarcoplasm.

A



B



abundant, NOS2 associates preferentially with intracellular membranes (Fig. 3B, middle). This particulate staining of NOS2 is more apparent at a higher magnification (Fig. 3B, right).

Effect of a \cdot NO donor on the caveolin levels in C2C12 myotubes

We intended to determine whether the diminution in the caveolin levels observed in the presence of the inflammatory insult were due to a transcriptional downregulation process induced by the LPS or IFN- γ themselves, or, alternatively, to the \cdot NO released by the activated myotubes. Remarkably, incubation of C2C12 myotubes with LPS/IFN- γ in the presence of the NOS2 inhibitors 1400W and nitro-Arg led to the downregulation of cav-1 and cav-2, and, at the same time, abrogated the expected diminution in the cav-3 levels (Fig. 4A). Moreover, addition of DETA-NONOate, a nitric-oxide-releasing compound, downregulates cav-3 but not cav-1 and cav-2. The possibility therefore exists that the decrease in the immunodetected cav-3 is the consequence of a transcriptional

Fig. 3. Localization of NOS2-GFP to the Golgi apparatus (A) and particulate immunofluorescence of NOS2-GFP both in myoblasts and myotubes (B). Live C2C12 myoblasts were grown on glass coverslips, transfected with a NOS2-GFP construct and incubated with the Golgi marker BODIPY-Texas red ceramide (A). In addition, C2C12 myoblasts and myotubes were grown on glass coverslips and transfected with GFP alone (left) or with a construct of NOS2 fused to the GFP reporter (right) (B). (B, far right) Magnification of myotubes transfected with a NOS2-GFP construct. The subcellular localization was analysed by laser confocal microscopy at an excitation wavelength of 488 nm. Scale bar, 10 μ M (bottom), 50 μ M (all others). In all cases, the position of the cell nuclei (blue) was obtained after staining with Hoechst and excitation at 405 nm.

or transductional downregulation triggered by nitric oxide itself. Treatment of myocytes with LPS/IFN- γ plus DETA-NONOate resulted in lower levels of cav-3 (Fig. 4A). The data suggest that the decrease in the cav-1 and cav-2 protein levels is due to the cytokines, whereas the decrease in the cav-3 protein levels is due to the \cdot NO resulting from NOS2 activity. Interestingly, this observation rationalizes our previous finding that cav-3 downregulation is somehow delayed compared with cav-1 and cav-2 (Fig. 1B). In order to gain further insight into the mechanism exerted by \cdot NO on the downregulation of the cav-3 protein content, C2C12 myotubes were incubated with 20 μ M 8-bromo-cGMP, a cell-permeable analog of cGMP (Fig. 4B). In the presence of neither 8-bromo-cGMP nor ODQ (a well-known inhibitor of soluble guanylate cyclase) could

we observe changes in the cav-1 and cav-2 levels (data not shown). Remarkably, the cav-3 protein levels were very marginally affected by this treatment, ruling out the \cdot NO-cGMP signaling pathway as the only mechanism leading to the downregulation that we previously observed. In addition, neither ODQ nor cycloheximide (CHX) were able to abrogate the downregulation of cav-3 observed in the presence of the \cdot NO donor DETA-NONOate (Fig. 4B). Likewise, ODQ alone induced no changes in the cav-3 levels (data not shown). In conclusion, the downregulation of the cav-3 by \cdot NO does not proceed through cGMP-derived pathways and does not seem to require de novo cellular synthesis of proteins.

Physical association between NOS2 and the three caveolin isoforms

Next, we attempted to investigate the interaction of cav-1, cav-2 and cav-3 with NOS2 in myotubes both by immunoprecipitation and through the purification of NOS2 using an affinity column (Fig. 5). When an extract from activated C2C12 myotubes is fractionated into soluble and

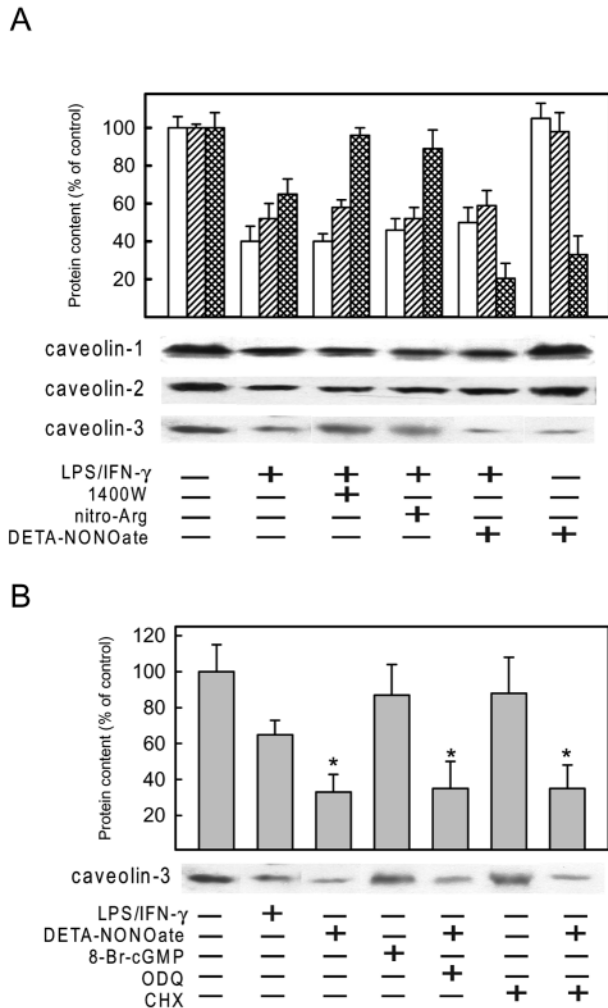


Fig. 4. Treatment of myotubes with $\cdot\text{NO}$ donors induce changes in the levels of cav-3, but not of cav-1 or cav-2. C2C12 myoblasts were differentiated into myotubes and incubated with LPS ($2 \mu\text{g ml}^{-1}$) plus IFN- γ (100 U ml^{-1}), the $\cdot\text{NO}$ donor DETA-NONOate ($100 \mu\text{M}$), the $\cdot\text{NO}$ inhibitors 1400W ($100 \mu\text{M}$) and nitro-Arg ($100 \mu\text{M}$) for 36 h (cav-1 and cav-2) or 48 h (cav-3) in different combinations. The cells were scraped and the changes in cav-1 (white bars), cav-2 (single-slashed bars) and cav-3 (double-slashed bars) protein levels were determined by immunodetection (A). In addition, activated C2C12 myotubes were incubated with the $\cdot\text{NO}$ donor DETA-NONOate, the lipophilic cGMP analog 8-bromo-cGMP ($20 \mu\text{M}$), with the soluble guanylate cyclase inhibitor ODQ ($10 \mu\text{M}$) or with cycloheximide (CHX; $10 \mu\text{M}$) in various combinations for 48 hours, and the levels of cav-3 were determined by immunodetection (B). In every case, the total amount of protein loaded was similar, as judged by β -tubulin quantification. * $P < 0.001$ vs the corresponding condition in the absence of $\cdot\text{NO}$ donor. Averaged results are shown, being representative of at least three independent experiments (\pm s.d.).

membranous fractions, approximately 80% of the NOS2 immunoreactivity remains in the soluble cytosolic fraction and about 20% remains associated with membranes (Fig. 5A). Interestingly, the membrane-associated NOS2 migrates with a slightly larger molecular mass than the soluble, cytosolic NOS2. We are currently exploring the putative post-translational modifications present in the inducible NOS in C2C12 muscle cells. As expected, cav-1, cav-2 and cav-3 all

associate with the particulate fraction of the cell (Fig. 5A). Immunoprecipitation of NOS2 from activated muscle cells was performed with a polyclonal serum (Fig. 5B). The enzyme appears to be associated strongly with cav-1 and CaM, and, to a lesser extent, with cav-2 and cav-3. Because NOS2 binds irreversibly to CaM, this finding indicates that, unlike endothelial NOS3, NOS2 can simultaneously associate with calmodulin and with caveolin, and preferentially with cav-1. In order to approximate the stoichiometry of this interaction we purified NOS2 by affinity chromatography on a 2',5'-ADP/Sepharose resin. Next, we loaded the appropriate amounts of both purified NOS2 and of a total lysate of activated C2C12 myotubes so that a similar band of NOS2 would be immunodetected (Fig. 5C). As observed in Fig. 5, cav-1, cav-2 and cav-3 purified with NOS2, although to very different extents. For instance, a significant amount of the total cellular cav-1 interacts with NOS2, whereas only minimal amounts of cav-2 and cav-3 associate with NOS2. The presence of more cav-1, but not cav-2 or cav-3, in association with NOS2 argues for a preferential interaction with this isoform. Support for a specific interaction with cav-1 is provided by the fact that significant amounts of cav-2 and cav-3 can still be immunodetected in the cellular lysate. These results establish that, although the three isoforms of caveolin associate with NOS2, there is a preferential binding to cav-1.

Depletion of caveolin using antisense oligonucleotides and effect of protein kinase inhibitors

In order to prove that the caveolin present within muscular cells associate with NOS2, hence reducing its enzymatic activity, we transfected C2C12 myotubes with antisense oligonucleotides for 8 hours. After this treatment, the culture medium was replaced and the cells were confronted with the proinflammatory stimulus for 36 hours. Nitrites that accumulated in the medium of mock and LPS/IFN- γ -treated cells were then determined (Fig. 6). Depletion of the endogenous cav-1 and cav-2 levels increased the amount of the $\cdot\text{NO}$ synthesized by approximately 52% and 50%, respectively, whereas depletion of endogenous cav-3 resulted in an increase in 24%. Addition of a mixture of the three antisense oligonucleotides resulted in an increase in 50% in the $\cdot\text{NO}$ synthesis. No changes were observed in the levels of NOS2 or β -tubulin as a consequence of the treatment. Immunoblotting analysis of the amount of cav-1, cav-2 and cav-3 protein resulting from the phosphorothioate treatment reveals that the C2C12 myotubes possess, in all cases, 60-70% of the caveolin protein content observed in untreated cells. Still, we cannot rule out the possibility that, after 24 hours of incubation with LPS/IFN- γ in the absence of antisense oligonucleotides, the cells partially recover from the treatment and increase their content in cav-1, cav-2 and cav-3. It must be noted that incubation with the antisense oligonucleotides specific for cav-1 frequently affected not only the cav-1 protein levels but also the cav-2 levels and vice versa, in agreement with the known hetero-association formed between cav-1 and cav-2 within cells. Thus, in accordance with the proposed role of caveolins as inhibitors of the activity of NOSs, reduction in the cav-1, cav-2 and (marginally) cav-3 levels proceeded with the concomitant increase in $\cdot\text{NO}$ synthesis.

Next, we activated the C2C12 myotubes with LPS/IFN- γ and tried to determine whether the downregulation in the cav-1 and

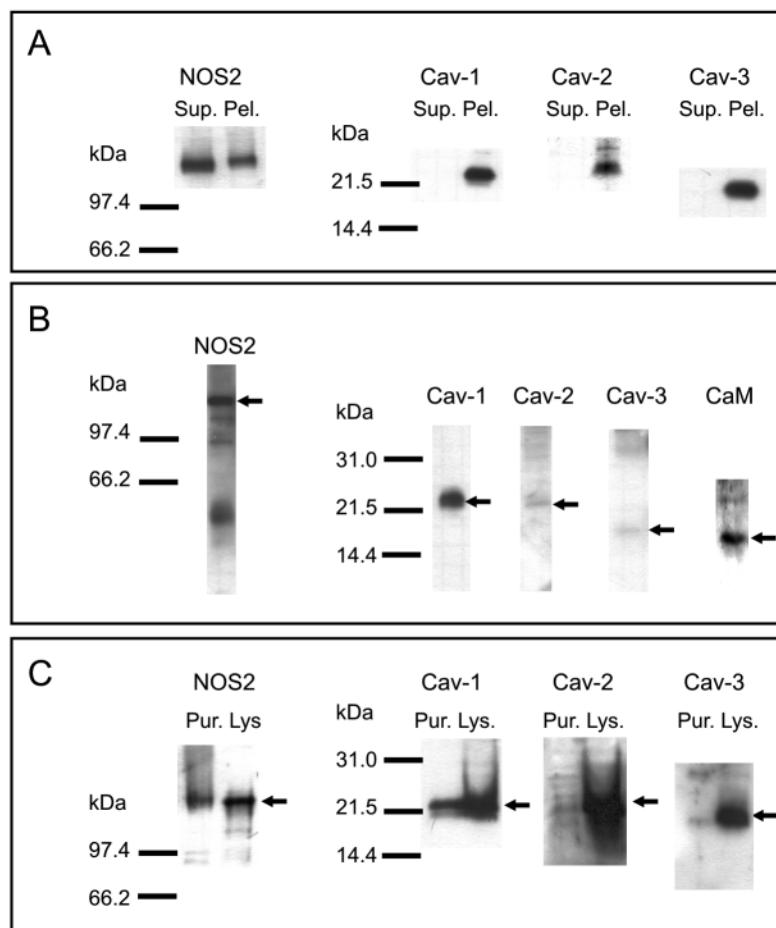


Fig. 5. Association of the three caveolin isoforms to NOS2 purified and immunoprecipitated from mouse C2C12 myotubes. Separation of the total lysate of LPS/IFN- γ -treated C2C12 myotubes into a soluble [Supernatant (Sup.)] or particulate [Pellet (Pel.)] fraction and analysis of the NOS2, cav-1, cav-2 and cav-3 distribution as judged by immunodetection (A). Additionally, NOS2 was immunoprecipitated from C2C12 myotubes treated with LPS/IFN- γ and the association with CaM, cav-1, cav-2 and cav-3 was determined (B). Finally, NOS2 was affinity purified using an ADP/Sepharose column (C). In this experiment, a lane was loaded with the amount of total cell lysate (Lys.) to give a similar NOS2 immunoreactivity to that of the purified sample (Pur.). Under this circumstance, the amount of cav-1, cav-2 and cav-3 that was retained bound to the purified NOS2 was compared with that present in the total lysate as determined by immunoblot (C).

LPS and IFN- γ into both wild-type and NOS2 knockout mice (Fig. 7). After 36 hours of treatment, both the NOS2^{+/+} and the NOS2^{-/-} animals effectively diminished their cav-1 protein levels immunodetected in skeletal muscle extracts. The wild-type animals downregulated their cav-3 levels as well. It is conceivable that the \cdot NO synthesized in a LPS/IFN- γ -treated muscle cell affects both the same cell and the neighboring cells in an autocrine and paracrine fashion, decreasing their cav-3 levels. Significantly, no attenuation in the cav-3 protein levels was observed in the muscle cells of knockout animals, reinforcing the notion that the NOS2-generated \cdot NO is responsible for the cav-3 protein decrease. This complete lack of effect of the cytokines in promoting the downregulation of the cav-3 protein levels in the knockout mice further supports the observations previously described for C2C12 myotubes.

Changes in cav-1 levels in other cell types

Other cell types respond to inflammatory stimuli by inducing NOS2 expression and synthesizing \cdot NO, so we investigated whether the cav-1 protein levels diminished in these cell types (Fig. 8). Liver cells isolated from mice injected with LPS/IFN- γ reduce their cav-1 protein levels significantly (Fig. 8), in parallel to the results obtained with the cultured C2C12 myotubes. The general downregulation of cav-1 in tissues that express NOS2 upon inflammation is strengthened by the results obtained for HepG2 cells and Raw 264.7 macrophages. In both cases, the endogenous cav-1 protein levels become downregulated in the presence of LPS/IFN- γ , hence reinforcing our previous findings. The cav-1 protein levels were almost undetectable in HepG2 cells at 32 hours after treatment whereas in Raw 264.7 macrophages (despite the low levels observed under basal conditions) no cav-1 band could be observed after 20 hours of treatment with the cytokines (Fig. 8).

Discussion

In this work, we describe the inhibitory association between NOS2 and caveolin in cell types that respond to

cav-2 levels could be blocked in the presence of protein kinase inhibitors (Fig. 6B). When the LPS/IFN- γ mixture was present, the cav-1 levels diminished to 40% of the initial protein levels, although this decrease could be partially abrogated in the presence of PD 98059, an inhibitor of the ERK pathway. By contrast, the C2C12 myotubes incubated with the LPS/IFN- γ mixture and challenged with none of wortmannin, LY 294002, SB 203580 and genistein could sustain the cav-1 protein levels observed in the control sample. Similar behavior was obtained when the cav-2 levels were determined. (data not shown). With this result in mind, we determined the concentration of nitrites that was present when PD 98059 was added to the cell culture (Fig. 6B). As expected, the restoration of the immunodetected cav-1 protein levels in myotubes in the presence of the LPS/IFN- γ mixture plus PD 98059 had produced a clear diminishment in the NOS2-derived \cdot NO (Fig. 6B, right). Hence, the sustained cav-1 and cav-2 levels even in the presence of the LPS/IFN- γ mixture are responsible for the abrogated activity of NOS2. It must be noted, nevertheless, that the addition of PD 98059 did not induce significant alterations in the NOS2 protein levels that were induced in the presence of the cytokines (data not shown).

Changes in the muscle caveolin levels in wild-type and NOS2 knockout animals

To explore the behavior of muscle cells in live animals and complement our studies carried out in cell cultures, we injected

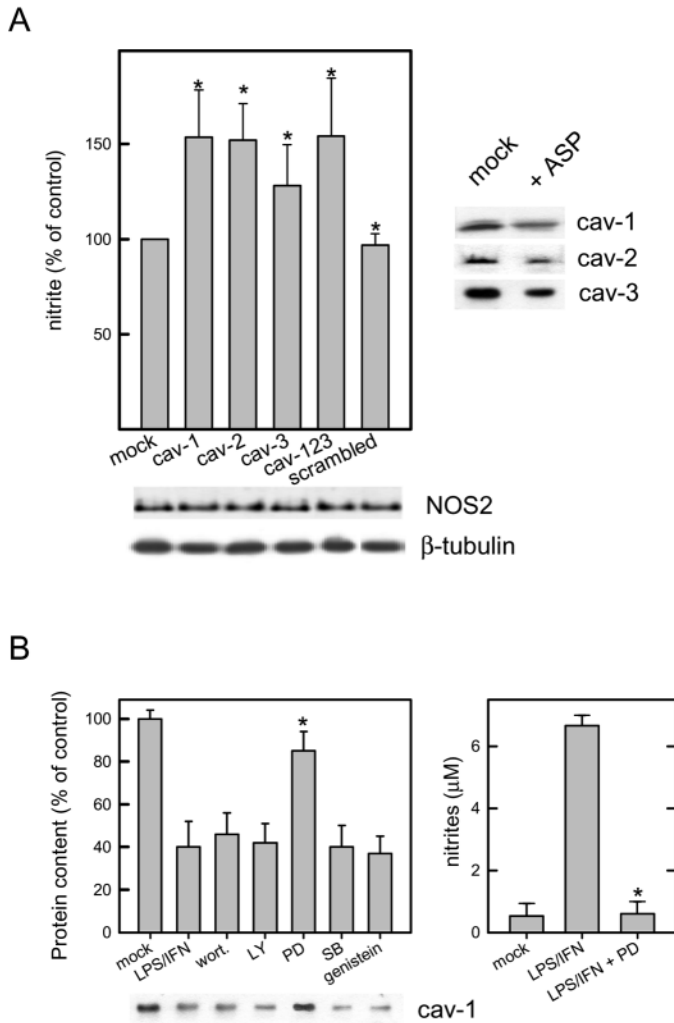


Fig. 6. Synthesis of $\cdot\text{NO}$ in mouse C2C12 myotubes treated with LPS/IFN- γ when incubated with antisense phosphorothioates (ASP) of cav-1, cav-2 and cav-3 (A), and abrogation of caveolin-1 downregulation by protein kinase inhibitors (B). C2C12 myotubes were treated for 8 hours with antisense phosphorothioate oligonucleotides complementary to the first 21 bases of the mRNA encoding cav-1, cav-2 and cav-3. After the treatment, the muscle cells were challenged with LPS/IFN- γ for 36 hours and the amount of $\cdot\text{NO}$ that accumulates was determined with the Griess assay. The antisense oligonucleotides (ASP) were added individually (cav-1, cav-2 and cav-3) or in combination (cav-123). A scrambled oligo corresponding to the cav-1 base sequence was also used as a control. The absence of changes in NOS2 and β -tubulin in each case is confirmed by immunodetection (A, bottom). The results shown are representative of ten individual experiments. In order to determine the pathway of downregulation followed by cav-1 and cav-2 in the presence of the LPS/IFN- γ mixture, the cells were incubated with various protein kinase inhibitors for 48 hours (B). Subsequently, the levels of cav-1 were determined by immunodetection. The concentration of nitrites in the supernatant in the presence of 10 μM Erk inhibitor PD was also determined (right). * $P < 0.001$ vs the LPS/IFN- γ condition. Error bars represent deviation from the average.

proinflammatory stimuli alongside the downregulation of caveolin that parallels the transcriptional induction of NOS2. The protein levels of cav-1, cav-2 and cav-3 all decreased

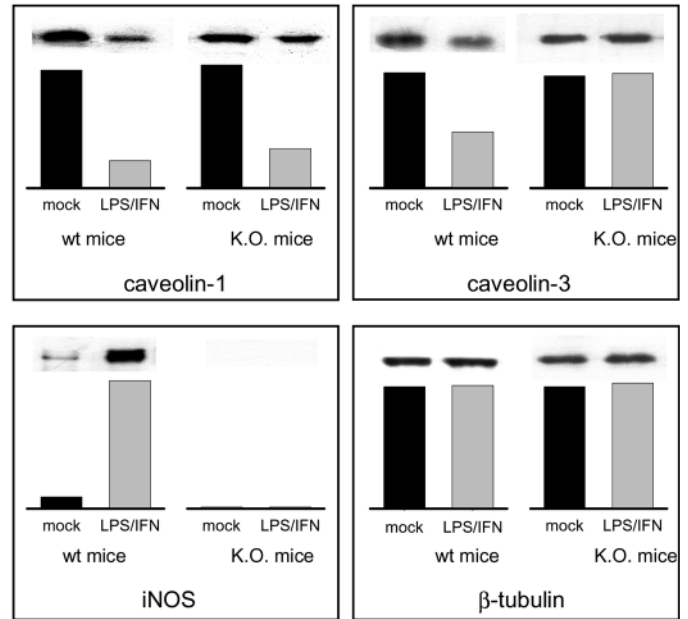


Fig. 7. Changes induced in NOS2, cav-1 and cav-3 levels in muscle (quadriceps) of wild-type (NOS2^{+/+}) and knock-out (NOS2^{-/-}) mice upon treatment with LPS/IFN- γ . The LPS/IFN- γ proinflammatory stimulus was maintained in animals for 36 hours and the muscular tissue was processed. The intensity of each immunodetected protein band was quantified using the UVI-band software and represented as a vertical bar chart. The results shown are representative of two individual experiments, with four mice used in each condition tested.

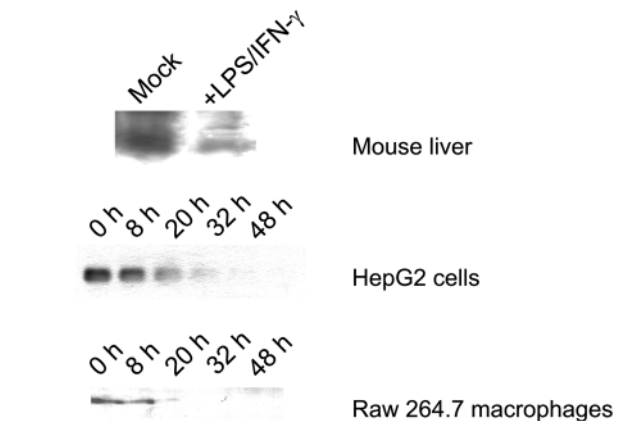


Fig. 8. Changes in the cav-1 levels observed with the LPS/IFN- γ proinflammatory stimulus in mouse hepatocytes, HepG2 cells and Raw 264.7 macrophages. Mice were injected with LPS (1.5 μg LPS g^{-1}) and IFN- γ (8 U g^{-1}), and the changes in the cav-1 levels were determined by immunodetection. HepG2 and Raw 264.7 were grown and challenged with the proinflammatory stimuli.

significantly after the treatment of muscle cells with LPS/IFN- γ . Whereas, cav-1 and cav-2 become downregulated in response to the cocktail of bacterial LPS and cytokine, cav-3 responded to the NOS2-derived $\cdot\text{NO}$ itself and became degraded/repressed. In fact, incubation of the C2C12 myotubes with the $\cdot\text{NO}$ donor DETA-NONOate triggered the decline in the cav-3 protein levels without affecting cav-1 and cav-2, suggesting a specific effect on this caveolin isoform.

We have demonstrated that, within skeletal muscle C2C12 myocytes, a membrane-associated subpopulation of NOS2 is present in direct contact with caveolin. This particulate NOS2 associates with both the sarcolemma (plasma membrane) of the myotubes and with intracellular membranes. Both skeletal muscle and the myotubes differentiated from the mouse C2C12 cell line are known to possess cav-1, cav-2 and cav-3 (Gath et al., 1999; Tang et al., 1996; Scherer et al., 1997; Song et al., 1996), and express NOS2 in abundance when challenged with LPS/IFN- γ (Williams et al., 1994; Stamler et al., 2001). We have immunoprecipitated and purified NOS2 from C2C12 myotubes, providing evidence of its association with calmodulin and with cav-1, and more marginally with cav-2 and cav-3. In addition, although the LPS/IFN- γ treatment led to a drop in the cav-1 protein levels, a significant amount of the remaining cellular cav-1 associate with NOS2. Interestingly, the major cellular path of NOS2 degradation is the 26S proteasome (Musial et al., 2001), and cav-1 overexpression has been reported to promote the degradation of NOS2 via the proteasome in human colon carcinoma cells (Felley-Bosco et al., 2000). Because the addition of peptides corresponding to the 'scaffolding domain' of cav-1 to purified NOS2 has been reported to abrogate its enzymatic activity (García-Cardena et al., 1997), the association between NOS2 and cav-1 that we observed in muscular tissues could reflect an inactive protein on its route towards proteasomal degradation. It remains to be established, therefore, which post-translational modifications give NOS2 the ability to associate with caveolar membranes. Interestingly, the NOS2 present in muscle cells migrated with a slightly higher molecular mass than its soluble counterpart. This piece of data is in accordance with the results obtained by Nathan and co-workers when working with macrophage NOS2 (Vodovotz et al., 1995), strongly implying that certain post-translational modifications that increase the total mass of NOS2 might be responsible for its targeting to membranes.

We report here that the association of NOS2 to cav-1 and, more marginally, to cav-2 and cav-3 impeded \cdot NO synthesis, as inferred from the augmented level of \cdot NO detected upon incubation with cav-1, cav-2 and cav-3 antisense phosphorothioate oligonucleotides. The comparable increase in \cdot NO synthesis that we observed for cav-1 and cav-2 antisense phosphorothioates, despite the fact that very little cav-2 protein is associated with immunoprecipitated and purified NOS2, very likely reflects the physical and functional interactions existing between cav-1 and cav-2 (Smart et al., 1999).

Additionally, we have shown that NOS2, which unlike endothelial NOS3 is known to bind irreversibly to calmodulin, associates with cav-1, cav-2 and cav-3, and becomes inactivated without releasing the CaM molecule. Therefore, the synthesis of \cdot NO achieved by both isoforms of NOS become modulated differently regarding their CaM-caveolin association.

The inability of NOS2 knockout but not wild-type mice to downregulate their cav-3 levels clearly indicates that nitric oxide exerts a specific transcriptional or transductional regulation of the cav-3 protein levels in muscular cells. A precedent for this is provided by experiments in which transient transfection of muscle cells with myogenin, a helix-loop-helix transcription factor, activated cav-3 reporter gene

expression, whereas Id2 overexpression inhibited cav-3 promoter activation by myogenin (Biederer et al., 2000). Our data suggest that nitric oxide might interfere with certain myogenic basic helix-loop-helix transcription factors such as myogenin, MyoD, Myf5 and MRF4. However, cardiomyocytes have a well documented interaction of cav-3 and endothelial NOS3, providing a precedent for the downregulation of the cav-3 levels. In rabbits raised under hypoxic conditions for 9 days, the myocardium responds increasing the amount of NOS3 and approximately halves the cellular levels of cav-3 (Shi et al., 2000).

By contrast, the diminution observed for cav-1 and cav-2 in C2C12 myotubes as a result of the addition of LPS/IFN- γ must be interpreted in terms of a signaling event resulting from the binding of these agents to their receptors. Regarding the downregulation of cav-1 in response to LPS/IFN- γ challenge, previous work has shown that activation of p42/p44 Erk and non-receptor tyrosine kinases such as Src and Abl are sufficient to accomplish this effect (Smart et al., 1999; Engelman et al., 1999). Indeed, a selective inhibitor of Erk activation impaired cav-1 and cav-2 loss under these conditions. Additionally, the close proximity of the *cav-1* and *cav-2* genes in mouse and humans (Fra et al., 2000), together with the observation that cav-2 is co-expressed with cav-1 in many tissues, forming hetero-oligomers, has lead to the proposal of their transcriptional co-regulation (Scherer et al., 1997; Smart et al., 1999; Fra et al., 2000). In this context, it must be noted that prolactin has been observed to regulate *cav-1* gene expression negatively in the mammary gland during lactation via a Ras-dependent mechanism, and, interestingly, the prolactin receptor is a cytokine receptor (Park et al., 2001).

In addition, our data indicate that the downregulation of the cellular cav-1 levels in the presence of LPS/IFN- γ might be a general phenomenon because, rather than being a unique feature of C2C12 myotubes, it is shared by other cell types, in agreement with the results reported by Lei and Morrison (Lei and Morrison, 2000).

Finally, a consideration should be made regarding the relative levels of NOS2 and caveolin in a particular cell. The results reported in this work, in addition to the description of the opposite regulation between NOS2 and caveolins, might be relevant to understand the fine tuning of NOS activity in those situations in which a moderate expression of NOS2 occurs, offering to the cell the possibility of selectively regulate and re-distribute, perhaps in specific microdomains, the local synthesis of \cdot NO. This subcellular targeting and localization of NOS2 might be responsible for its activation state, because both cav-1 and the muscle-specific cav-3 isoform are predominantly associated to the sarcolemma. This situation might be of interest in those cases in which \cdot NO is mainly involved in signaling and not in other functions that require a high-output production. Unraveling the biological effects of caveolin-targeted NOS2 subcellular localization might provide new insights into the broad spectrum on NOS2 inducibility among cells, distinct from those directly involved in host defense.

We thank M. Lorenzo (Universidad Complutense de Madrid) for providing us with the mouse myoblast C2C12 cell line, and Á. M. del Pozo, A. Saborido (Universidad Complutense de Madrid), M. Á. Alonso (CBM, Madrid) and S. Lamas (CIB, Madrid) for critical

reviews of the manuscript. We are also indebted to R. Nieto for excellent technical assistance.

References

- Adams, V., Jiang, H., Yu, J., Mobius-Winkler, S., Fiehn, E., Linke, A., Weigl, C., Schuler, G. and Hambrecht, R. (1999). Apoptosis in skeletal myocytes of patients with chronic heart failure is associated with exercise intolerance. *J. Am. Coll. Cardiol.* **33**, 959-965.
- Biederer, C. H., Ries, S. J., Moser, M., Florio, M., Israel, M. A., McCormick, F. and Buettner, R. (2000). The basic helix-loop-helix transcription factors myogenin and Id2 mediate specific induction of caveolin-3 gene expression during embryonic development. *J. Biol. Chem.* **275**, 26245-26251.
- Bogdan, C. (2001). Nitric oxide and the immune response. *Nat. Immunol.* **2**, 907-916.
- Cho, H. J., Xie, Q. W., Calaycay, J., Mumford, R. A., Swiderek, K. M., Lee, T. D. and Nathan, C. (1992). Calmodulin is a subunit of nitric oxide synthase from macrophages. *J. Exp. Med.* **176**, 599-604.
- Conejo, R., Valverde, A. M., Benito, M. and Lorenzo, M. (2001). Insulin produces myogenesis in C2C12 myoblasts by induction of NF-kappaB and downregulation of AP-1 activities. *J. Cell. Physiol.* **186**, 82-94.
- Engelman, J. A., Zhang, X. L., Razani, B., Pestell, R. G. and Lisanti, M. P. (1999). p42/44 MAP kinase-dependent and -independent signaling pathways regulate caveolin-1 gene expression. Activation of Ras-MAP kinase and protein kinase A signaling cascades transcriptionally down-regulates caveolin-1 promoter activity. *J. Biol. Chem.* **274**, 32333-32341.
- Felley-Bosco, E., Bender, F. C., Courjault-Gautier, F., Bron, C. and Quest, A. F. (2000). Caveolin-1 down-regulates inducible nitric oxide synthase via the proteasome pathway in human colon carcinoma cells. *Proc. Natl. Acad. Sci. USA* **97**, 14334-14339.
- Feron, O., Saldana, F., Michel, J. B. and Michel, T. (1998). The endothelial nitric-oxide synthase-caveolin regulatory cycle. *J. Biol. Chem.* **273**, 3125-3128.
- Fra, A. M., Pasqualetto, E., Mancini, M. and Sitia, R. (2000). Genomic organization and transcriptional analysis of the human genes coding for caveolin-1 and caveolin-2. *Gene* **243**, 75-83.
- García-Cardena, G., Martasek, P., Masters, B. S., Skidd, P. M., Couet, J., Li, S., Lisanti, M. P. and Sessa, W. C. (1997). Dissecting the interaction between nitric oxide synthase (NOS) and caveolin. Functional significance of the NOS caveolin binding domain in vivo. *J. Biol. Chem.* **272**, 25437-25440.
- Gath, I., Closs, E. I., Godtel-Armbrust, U., Schmitt, S., Nakane, M., Wessler, I. and Förstermann, U. (1996). Inducible NO synthase II and neuronal NO synthase I are constitutively expressed in different structures of guinea pig skeletal muscle: implications for contractile function. *FASEB J.* **10**, 1614-1620.
- Gath, I., Ebert, J., Godtel-Armbrust, U., Ross, R., Reske-Kunz, A. B. and Förstermann, U. (1999). NO synthase II in mouse skeletal muscle is associated with caveolin 3. *Biochem. J.* **340**, 723-728.
- Gratton, J. P., Fontana, J., O'Connor, D. S., Garcia-Cardena, G., McCabe, T. J. and Sessa, W. C. (2000). Reconstitution of an endothelial nitric-oxide synthase (eNOS), hsp90, and caveolin-1 complex in vitro. Evidence that hsp90 facilitates calmodulin stimulated displacement of eNOS from caveolin-1. *J. Biol. Chem.* **275**, 22268-22272.
- Hibbs, J. B., Jr, Taintor, R. R., Vavrin, Z. and Rachlin, E. M. (1988). Nitric oxide: a cytotoxic activated macrophage effector molecule. *Biochem. Biophys. Res. Commun.* **157**, 87-94.
- Kunciewicz, T., Balakrishnan, P., Snuggs, M. B. and Kone, B. C. (2001). Specific association of nitric oxide synthase-2 with Rac isoforms in activated murine macrophages. *Am. J. Physiol. Renal Physiol.* **281**, F326-F336.
- Lei, M. G. and Morrison, D. C. (2000). Differential expression of caveolin-1 in lipopolysaccharide-activated murine macrophages. *Infect. Immun.* **68**, 5084-5089.
- Luetterforst, R., Stang, E., Zorzi, N., Carozzi, A., Way, M. and Parton, R. G. (1999). Molecular characterization of caveolin association with the Golgi complex: identification of a cis-Golgi targeting domain in the caveolin molecule. *J. Cell Biol.* **145**, 1443-1459.
- MacMicking, J., Xie, Q. W. and Nathan, C. (1997). Nitric oxide and macrophage function. *Annu. Rev. Immunol.* **15**, 323-350.
- Musial, A. and Eissa, N. T. (2001). Inducible nitric-oxide synthase is regulated by the proteasome degradation pathway. *J. Biol. Chem.* **276**, 24268-24273.
- Navarro-Lérida, I., Álvarez-Barrientos, A., Gavilanes, F. and Rodríguez-Crespo, I. (2002). Distance-dependent cellular palmitoylation of de-novo-designed sequences and their translocation to plasma membrane subdomains. *J. Cell Sci.* **115**, 3119-3130.
- Park, C. S., Park, R. and Krishna, G. (1996). Constitutive expression and structural diversity of inducible isoform of nitric oxide synthase in human tissues. *Life Sci.* **59**, 219-225.
- Park, D. S., Lee, H., Riedel, C., Hulit, J., Scherer, P. E., Pestell, R. G. and Lisanti, M. P. (2001). Prolactin negatively regulates caveolin-1 gene expression in the mammary gland during lactation, via a Ras-dependent mechanism. *J. Biol. Chem.* **276**, 48389-48397.
- Ratovitski, E. A., Alam, M. R., Quick, R. A., McMillan, A., Bao, C., Kozlovsky, C., Hand, T. A., Johnson, R. C., Mains, R. E., Eipper, B. A. et al. (1999a). Kalirin inhibition of inducible nitric-oxide synthase. *J. Biol. Chem.* **274**, 993-999.
- Ratovitski, E. A., Bao, C., Quick, R. A., McMillan, A., Kozlovsky, C. and Lowenstein, C. J. (1999b). An inducible nitric-oxide synthase (NOS)-associated protein inhibits NOS dimerization and activity. *J. Biol. Chem.* **274**, 30250-30257.
- Riede, U. N., Förstermann, U. and Drexler, H. (1998). Inducible nitric oxide synthase in skeletal muscle of patients with chronic heart failure. *J. Am. Coll. Cardiol.* **32**, 964-969.
- Ringheim, G. E. and Pan, J. (1995). Particulate and soluble forms of the inducible nitric oxide synthase are distinguishable at the amino terminus in RAW 264.7 macrophage cells. *Biochem. Biophys. Res. Commun.* **210**, 711-716.
- Rodríguez-Crespo, I., Nishida, C. R., Knudsen, G. M. and Ortiz de Montellano, P. R. (1999). Mutation of the five conserved histidines in the endothelial nitric-oxide synthase hemoprotein domain. No evidence for a non-heme metal requirement for catalysis. *J. Biol. Chem.* **274**, 21617-21624.
- Scherer, P. E., Lewis, R. Y., Volonte, D., Engelman, J. A., Galbati, F., Couet, J., Kohtz, D. S., van Donselaar, E., Peters, P. and Lisanti, M. P. (1997). Cell-type and tissue-specific expression of caveolin-2. Caveolins 1 and 2 co-localize and form a stable hetero-oligomeric complex in vivo. *J. Biol. Chem.* **272**, 29337-29346.
- Shi, Y., Pritchard, K. A., Jr, Holman, P., Rafiee, P., Griffith, O. W., Kalyanaraman, B. and Baker, J. E. (2000). Chronic myocardial hypoxia increases nitric oxide synthase and decreases caveolin-3. *Free Radic. Biol. Med.* **29**, 695-703.
- Smart, E. J., Graf, G. A., McNiven, M. A., Sessa, W. C., Engelman, J. A., Scherer, P. E., Okamoto, T. and Lisanti, M. P. (1999). Caveolins, liquid-ordered domains, and signal transduction. *Mol. Cell. Biol.* **19**, 7289-7304.
- Song, K. S., Scherer, P. E., Tang, Z., Okamoto, T., Li, S., Chafel, M., Chu, C., Kohtz, D. S. and Lisanti, M. P. (1996). Expression of caveolin-3 in skeletal, cardiac, and smooth muscle cells. Caveolin-3 is a component of the sarcolemma and co-fractionates with dystrophin and dystrophin-associated glycoproteins. *J. Biol. Chem.* **271**, 15160-15165.
- Stamler, J. S. and Meissner, G. (2001). Physiology of nitric oxide in skeletal muscle. *Physiol. Rev.* **81**, 209-237.
- Tang, Z., Scherer, P. E., Okamoto, T., Song, K., Chu, C., Kohtz, D. S., Nishimoto, I., Lodish, H. F. and Lisanti, M. P. (1996). Molecular cloning of caveolin-3, a novel member of the caveolin gene family expressed predominantly in muscle. *J. Biol. Chem.* **271**, 2255-2261.
- Tews, D. S. and Goebel, H. H. (1998). Cell death and oxidative damage in inflammatory myopathies. *Clin. Immunol. Immunopathol.* **87**, 240-247.
- van't Hof, R. J., Armour, K. J., Smith, L. M., Armour, K. E., Wei, X. Q., Liew, F. Y. and Ralston, S. H. (2000). Requirement of the inducible nitric oxide synthase pathway for IL-1-induced osteoclastic bone resorption. *Proc. Natl. Acad. Sci. USA* **97**, 7993-7998.
- Vodovotz, Y., Russell, D., Xie, Q. W., Bogdan, C. and Nathan, C. (1995). Vesicle membrane association of nitric oxide synthase in primary mouse macrophages. *J. Immunol.* **154**, 2914-2925.
- Williams, G., Brown, T., Becker, L., Prager, M. and Giroir, B. P. (1994). Cytokine-induced expression of nitric oxide synthase in C2C12 skeletal muscle myocytes. *Am. J. Physiol.* **267**, R1020-R1025.